Received: 20 June 2018 | Accepted: 11 October 2018

DOI: 10.1111/nrm.12202

WILEY Natural Resource Modeling

Dynamics of coral reef models in the presence of parrotfish

Haniyeh Fattahpour[1] | **Hamid R.Z. Zangeneh**[1] | **Hao Wang**[2]

[1]Department of Mathematical Sciences, Isfahan University of Technology, Isfahan, Iran

[2]Department of Mathematical and Statistical Sciences, University of Alberta, Edmonton, Alberta, Canada

Correspondence
Hamid R.Z. Zangeneh, Department of Mathematical Sciences, Isfahan University of Technology, Isfahan 84156-83111, Iran.
Email: hamidz@cc.iut.ac.ir

Abstract

The decline of coral reefs characterized by macroalgae increase has been a global threat. We consider a slightly modified version of an ordinary differential equation (ODE) model proposed in Blackwood, Hastings, and Mumby [Theor. Ecol. 5 (2012), pp. 105–114] that explicitly considers the role of parrotfish grazing on coral reef dynamics. We perform complete stability, bifurcation, and persistence analysis for this model. If the fishing effort (f) is in between two critical values f_0 and f_1, then the system has a unique interior equilibrium, which is stable if $f_0 < f < f_1$ and unstable if $f_1 < f < f_0$. If f is less (more) than these critical values, then the system has up to two (zero) interior equilibria. Also, we develop a more realistic delay differential equation (DDE) model to incorporate the time delay and treating it as the bifurcation parameter, and we prove that Hopf bifurcation about the interior equilibria could occur at critical time delays, which illustrate the potential importance of the inherent time delay in a coral reef ecosystem.

Recommendations for Resource Managers

- One serious threat to coral reefs is overfishing of grazing species, including high level of algal abundance. Fishing alters the entire dynamics of a reef (Hughes, Baird, & Bellwood, 2003), for which the coral cover was predicted to decline rapidly (Mumby, 2006). One major issue is to reverse and develop appropriate management to increase or maintain coral resilience.
- We have provided a detailed local and global analysis of model (Blackwood, Hastings, & Mumby, 2012) and

obtained an ecologically meaningful attracting region, for which there is a chance of stable coexistence of coral–algal–fish state.

- The healthy reefs switch to unhealthy state, and the macroalgae–parrotfish state becomes stable as the fishing effort increases through some critical values. Also, for some critical time delays, a switch between healthy and unhealthy reef states occurs through a Hopf bifurcation, which can only appear in the delay differential equation (DDE) model. Eventually, for large enough time delay, oscillations appear and an unhealthy state occurs.

KEYWORDS

coral reef, delay differential equation, Hopf bifurcation, ordinary differential equation, stability

1 | INTRODUCTION

Global diversity and quality of life of millions of people living in tropical coastal regions have been endangered by frequency and scale of human impacts on the health of world's coral reefs (cf., Mumby, Hastings, & Edwards, 2007; Pandolfi, Bradbury, & Sala, 2003). The worldwide decline of coral reefs, which is characterized by macroalgae increase, has demonstrated an urgent need to scale up the management effort based on improved understanding of ecological dynamics that underlies the reef resilience (cf., Bellwood, Hughes, Folke, & Nystrom, 2004).

Mumby et al. (2007) introduced a model with grazing that shows a coral reef ecosystem that may lose resilience and shift to coral-depleted state through reductions in grazing intensity, which has been analyzed mathematically in Li, Wang, Zhang, and Hastings (2014). This model has been extended by Blackwood et al. (2012) in the explicit incorporation of parrotfish abundance. It has been hypothesized that excessive fishing pressure is a potential cause of hysteresis (cf., Li et al., 2014). Motivated by these papers, our aim is to consider a modified version of the ordinary differential equation (ODE) model in Blackwood et al. (2012) and to determine explicitly the role of parrotfish abundance on grazing intensity and implement management on the coral reef system.

The analysis of ecological systems often focuses on their asymptotic behavior, but it is important to understand the role of transient behavior. The inherent delay effect has been considered to be important on coral–algae–parrotfish interactions (cf., Blackwood & Hastings, 2011), in which the authors discussed the effect of time delays on the basis of attraction of stable equilibria, which in turn may have important management implications in coral reef as well as other ecosystems exhibiting similar dynamical behavior. Algal turfs will not be bloomed immediately after macroalgae are grazed by parrotfish. To account for the time delay, and accordingly the time that affect the natural system, we develop and analyze a more realistic delay differential equation (DDE) model by treating the time delay as the bifurcation parameter.

We consider the fishing effort and time delay as the bifurcation parameter and analyze the local stability of equilibria for the DDE model.

The paper is organized as follows. In Section 2, we present our basic assumptions and the ODE model. In Section 3, we consider the existence, stability, and bifurcation of all possible equilibria of the system and show the uniform persistence result. In Section 4, we construct a DDE model to account for the role of time delay in the coral reef dynamics. We prove that the Hopf bifurcation can occur about the unique interior equilibria. In Section 5, we present representative numerical simulations to support our analytical results. Finally, in Section 6, we conclude our results and provide biological interpretations.

2 | THE MODEL AND BASIC ASSUMPTIONS

In this section, we consider the following modified version of the ODE model presented in Blackwood et al. (2012):

$$\begin{cases} \frac{dM}{dt} = aMC - \frac{g(P)M}{1+M+T} + \gamma MT, \\ \frac{dC}{dt} = rTC - dC - aMC, \\ \frac{dT}{dt} = \frac{g(P)M}{1+M+T} - \gamma MT - rTC + dC, \\ \frac{dP}{dt} = sP\left(1 - \frac{P}{\beta K(C)}\right) - fP. \end{cases} \tag{1}$$

(i) We assume that a particular region of the seabed is covered entirely by macroalgae (M), coral (C), and algal turfs (T) so that $M + C + T$ is kept constant, which by a rescaling we may assume that $M + C + T = 1$. Therefore, the fraction of algal turfs is defined by $T = 1 - M - C$ and consequently $\frac{dT}{dt} = -\frac{dM}{dt} - \frac{dC}{dt}$.

(ii) It is assumed that corals recruit and overgrow algal turfs at a rate r, they have a natural mortality rate of d, are overgrown by macroalgae at a rate a, and macroalgae spread vegetatively over algal turfs at a rate γ. Space freed by coral mortality is assumed to be recolonized by algal turfs. Additionally, $M/(1 + M + T)$ is simply the proportion of grazing that affects macroalgae.

(iii) Changes in parrotfish abundance, P, are modeled as logistic growth with an intrinsic rate of growth s and a time varying carrying capacity such that β is the maximum carrying capacity and $0 < K(C) \leq 1$ is a nondimensional term that limits carrying capacity of parrotfish as a function of coral cover. We have simplified the model by the assuming that parrotfish lacks adequate refugia, likely as a result of hurricane impacts resulting in a positive relationship between parrotfish carrying capacity and coral growth. Thus, we use the carrying capacity that is defined as $K(C) = 1 - kC$, where $0 \leq k < 1$, so that there is a short-term positive response to coral recruitment. Furthermore, it is assumed that mortality resulting from fishing effort is held at a constant level $f \geq 0$.

(iv) Grazing intensity varies depending on parrotfish abundance so that the grazing is defined by as a function $g(P)$. It is assumed that the grazing intensity is proportional to parrotfish abundance, relative to its maximum carrying capacity, or $g(P) = \frac{\alpha P}{\beta}$, where α is a positive

constant. It is natural to let $\alpha = g_{\max}$, where $g_{\max}$ is the maximum possible grazing intensity and for simplicity it is assumed to be equal one. Thus, $g(P) = \frac{P}{\beta}$ and this formulation guarantees that the grazing intensity will arrive at its maximum only if fishing effort is eliminated ($f = 0$). For simplicity, we scale parrotfish abundance and introduce the nondimensional variable $\tilde{P}$ to be parrotfish abundance relative to its maximum carrying capacity, or $\tilde{P} = \frac{P}{\beta}$. Substituting this in the last equation of (1) leaves with $\frac{d\tilde{P}}{dt} = s\tilde{P}(1 - \frac{\tilde{P}}{K(C)}) - f\tilde{P}$, and the grazing function is now given by $g(P) = \tilde{P}$. For simplicity in notation, we set $\tilde{P} =: P$.

From the aforementioned and setting $M \coloneqq x$, $C \coloneqq y$, and $P \coloneqq z$, equations of the model dynamics are given by the following nonlinear system of ODEs:

$$\begin{cases} \frac{dx}{dt} = x\left[\gamma - \gamma x + (a - \gamma)y - \frac{z}{2-y}\right] \coloneqq xF(x, y, z), \\ \frac{dy}{dt} = y[(r - d) - (r + a)x - ry] \coloneqq yG(x, y, z), \\ \frac{dz}{dt} = z\left[(s - f) - \frac{sz}{1 - ky}\right] \coloneqq zH(x, y, z). \end{cases} \tag{2}$$

The brief description of the parameter selection and parameter values can be found in Blackwood et al. (2012) and Mumby et al. (2007), in which the authors listed the parameter values as follows:

$$a = 0.1, \quad d = 0.44, \quad s = 0.49, \quad \gamma = 0.8, \quad r = 1, \quad 0 \le f < 0.49, \quad 0 \le k < 1.$$

Here, we only assume that all parameters are positive and satisfy the following assumptions:

$$a < \gamma < r + a, \quad r > d, \quad 0 < \frac{s - f}{s} < 2\gamma, \quad 0 \le k < 1. \tag{3}$$

For convenience, we denote $\mu \coloneqq \frac{s-f}{s}$.

3 | EQUILIBRIA: STABILITY AND BIFURCATION

In this section, we find all possible equilibria and consider their stabilities. By considering the nullclines of the system (2), we could easily find the following equilibria:

- *The trivial state*: $O = (0, 0, 0)$.
- *The axial states*: $R = (0, 0, \mu)$, $N = (0, \frac{r-d}{r}, 0)$, $Q = (1, 0, 0)$.
- *The boundary states*: $D = (0, \frac{r-d}{r}, \frac{\mu(r(1-k)+kd)}{r})$, $F = (1 - \frac{\mu}{2\gamma}, 0, \mu)$. Here, we notice that there is another boundary state $G = (\frac{ra - ad + d\gamma}{ar + a^2 - a\gamma}, \frac{-\gamma(a+d)}{a^2 + ar - a\gamma}, 0)$, which is not in the first positive octant, so it is ignored here.

- *The interior steady state*: $E^* = (x^*, y^*, z^*)$ is the solution of $F(x, y, z) = G(x, y, z) = H(x, y, z) = 0$, so that x^* and z^* satisfy

$$x^* = \frac{r-d}{r+a} - \frac{ry^*}{r+a}, \quad z^* = \mu(1 - ky^*). \tag{4}$$

and y^* is a solution of the following quadratic equation:

$$K(y) := \mathcal{A}y^2 + \mathcal{B}y + C, \tag{5}$$

where

$$\begin{aligned} \mathcal{A} &= -a(r + a - \gamma), \\ \mathcal{B} &= -\gamma(a + d) + 2a(r + a - \gamma) - \mu k(r + a), \\ C &= 2\gamma(a + d) - \mu(r + a). \end{aligned}$$

This solution should belong to the interval $(0, \frac{r-d}{r})$, because otherwise $x^* < 0$. Notice that, under the assumption (3), the axial points (R, N, and Q) and the boundary points (D and F) always exist. Now, let us define the following quantities:

$$\mu_0 := \frac{a(r^2 - d^2) + (r + d)\gamma d}{r^2 + rkd - r^2 k}, \quad \mu_1 := \frac{2\gamma(a + d)}{r + a}. \tag{6}$$

Notice that μ_0 is a function of k and $\mu_0 = \mu_1$ for $k = k_0 := \frac{1}{2} - \frac{a(r-d)(a+r-\gamma)}{2\gamma r(a+d)}$. Also, $\mu_1 < \mu_0$ for $0 \le k_0 < k$ and $0 \le \mu_0 < \mu_1$ for $0 \le k < k_0$.

In the following, we find conditions of interior equilibrium.

First, we note that

$$\begin{aligned} K(0) &= (r + a)(\mu_1 - \mu), \\ K\left(\tfrac{r-d}{r}\right) &= (r + a)\left(1 - \tfrac{k(r-d)}{r}\right)(\mu_0 - \mu), \end{aligned}$$

where μ_0 and μ_1 are defined in (6). Let $Y_{\max}$ be the maximum point of $K(y)$ and $\Delta = \mathcal{B}^2 - 4\mathcal{A}C$.

We need to consider the following cases separately:

Case (I) $0 < \mu_1 < \mu_0$: Then, there can be three different scenarios:

- **(i)** $0 < \mu < \mu_1 < \mu_0$: In this case, $K(0) > 0$ and $K(\frac{r-d}{r}) > 0$. Then, depending on the position of $Y_{\max}$, there are three possibilities:
  - **(a)** $0 \le Y_{\max} \le \frac{r-d}{r}$: Then, $K(y) > \max(K(0), K(\frac{r-d}{r})) > 0$.
  - **(b)** $Y_{\max} > \frac{r-d}{r}$: Then, $K(y)$ is increasing in $(0, \frac{r-d}{r})$ and therefore $K(y) > K(0) > 0$.
  - **(c)** $Y_{\max} < 0$: Then, $K(y)$ is decreasing in $(0, \frac{r-d}{r})$ and therefore $K(y) > K(\frac{r-d}{r}) > 0$. This implies that $K(y)$ is positive on $(0, \frac{r-d}{r})$ and therefore there is no interior equilibrium.

(ii) $0 < \mu_1 < \mu < \mu_0$: In this case, $K(0) < 0$ and $K(\frac{r-d}{r}) > 0$, then $K(y)$ has at least one solution in $(0, \frac{r-d}{r})$. Depending on the position of $Y_{\max}$, there are two possibilities:

(a) $0 < Y_{\max} < \frac{r-d}{r}$.

(b) $Y_{\max} \geq \frac{r-d}{r}$. In either case, $K(y)$ has two positive solutions from which only the smaller solution, $y^* = \frac{-\mathcal{B} - \sqrt{\Delta}}{2\mathcal{A}}$, is in $(0, \frac{r-d}{r})$.

(iii) $0 < \mu_1 < \mu_0 < \mu$: In this case, $K(0) < 0$ and $K(\frac{r-d}{r}) < 0$. Again there are three different possibilities:

(a) $Y_{\max} \leq 0$ or

(b) $Y_{\max} \geq \frac{r-d}{r}$. In these two cases, $K(y)$ is monotone on $(0, \frac{r-d}{r})$ and therefore there is no solution in the interval of interest.

(c) $0 < Y_{\max} < \frac{r-d}{r}$: Notice that this holds only if $\mu_* < \mu < \mu^*$, where

$$\mu_* =: \frac{(3a+d)\gamma - 2a(r+a)}{k(r+a)}, \quad \mu^* := \frac{a\gamma(r+d) + d(r+a)(-2a+\gamma)}{kr(r+a)}.$$

But $\mu^* > \mu_* > 0$ always holds, as by hypothesis (3), $2a(r-d)[-\gamma + r + a] > 0$. Furthermore, μ^*, μ_*, and μ_0 are functions of parameter k. μ^* and μ_* are decreasing in k, whereas μ_0 is increasing in k. Also, it can be shown that $\mu^*(1) < \mu_1$. Therefore, depending on the value of Δ, $K(y)$ can have up to two solutions in $(0, \frac{r-d}{r})$.

Case (II) $0 < \mu_0 < \mu_1$:

As in Case (I) and by similar argument, we can conclude the following:

(i) $\mu < \mu_0 < \mu_1$: $K(y)$ has no solution in interval $(0, \frac{r-d}{r})$.

(ii) $0 < \mu_0 < \mu < \mu_1$: $K(y)$ has a unique positive solution $y^* = \frac{-\mathcal{B} + \sqrt{\Delta}}{2\mathcal{A}}$ in the interval $(0, \frac{r-d}{r})$.

(iii) $\mu_0 < \mu_1 < \mu$: $K(y)$ can have up to two solutions in the interval $(0, \frac{r-d}{r})$.

We summarize the above discussion in the following proposition.

Proposition 1.

(a) If $0 < \mu_1 < \mu < \mu_0$ or $0 < \mu_0 < \mu < \mu_1$, the system (2) has a unique interior equilibrium.

(b) If $\mu < \mu_1 < \mu_0$ or $\mu < \mu_0 < \mu_1$, the system (2) has no interior equilibria.

(c) If $\mu_1 < \mu_0 < \mu$ or $\mu_0 < \mu_1 < \mu$, the system (2) can have up to two interior equilibria.

Now, we study the local stability of the trivial state O, the axial states R, N, Q, and the boundary states D and F by calculating the eigenvalues of the Jacobian matrix of the system (2)

$$J_{(x,y,z)} = \begin{pmatrix} F + xF_x & xF_y & xF_z \\ yG_x & G + yG_y & yG_z \\ zH_x & zH_y & H + zH_z \end{pmatrix}$$

about different equilibria. By looking at eigenvalues of J, we can easily check that O is an unstable node, whereas the axial solutions R, N, and Q are always a saddle. Now, we consider the boundary points:

- *Boundary point D*. Eigenvalues are $\lambda_1 = \frac{(r(1-k)+kd)}{(r+d)}(\mu_0 - \mu)$, $\lambda_2 = -(r-d)$, and $\lambda_3 = -s\mu$. Under the assumption (3), λ_2 and λ_3 are always negative. If $\mu_0 < \mu$, $\lambda_1 < 0$, and D is a stable node, if $0 < \mu < \mu_0$, $\lambda_1 > 0$ and it is unstable. It can be easily checked that the system undergoes a transcritical bifurcation about the boundary point D as μ passes through μ_0.
- *Boundary point F*. Eigenvalues are $\lambda_1 = -\gamma + \frac{\mu}{2}$, $\lambda_2 = (\frac{r+a}{2\gamma})(\mu - \mu_1)$, and $\lambda_3 = -s\mu$. Under the assumption (3), λ_1 and λ_3 are always negative. F is a stable node, if $\mu_1 > \mu$, $\lambda_2 < 0$ and it is unstable if $0 < \mu_1 < \mu$, $\lambda_2 > 0$. It can be easily seen that the system (2) undergoes a transcritical bifurcation as μ passes through μ_1.

Next, we analyze the stability of interior equilibrium point $E^* = (x^*, y^*, z^*)$. About E^*, the Jacobian matrix J takes the form

$$J_{E^*} = \begin{pmatrix} x^*F_x & x^*F_y & x^*F_z \\ y^*G_x & y^*G_y & y^*G_z \\ z^*H_x & z^*H_y & z^*H_z \end{pmatrix}$$

and its eigenvalues satisfy

$$\lambda^3 + A\lambda^2 + B\lambda + C = 0, \tag{7}$$

where

$$\begin{aligned} A &:= \gamma x^* + ry^* + s\mu, \\ B &:= \gamma r x^* y^* + x^* y^* (a + r)\left(a - \gamma - \tfrac{z^*}{(2-y^*)^2}\right) + s\mu(\gamma x^* + ry^*), \\ C &:= s\mu x^* y^* \left[r\gamma + (a + r)(a - \gamma) - \tfrac{z^*(r+a)}{(2-y^*)^2}\right) + \tfrac{k(r+a)\mu}{(2-y^*)}\Bigg]. \end{aligned}$$

To determine the type of stability of E^*, we determine the sign of A, C, and $AB - C$. Here, it is clear that $A > 0$. From the algebraic equation $F(x^*, y^*, z^*) = 0$, we have $\frac{z^*}{2-y^*} = \gamma - \gamma x^* + (a - \gamma)y^*$ and from $G(x^*, y^*, z^*) = 0$, we have $x^* = \frac{r - d - ry^*}{r + a}$, then C can be written as

$$C = \frac{s\mu x^* y^*}{2 - y^*}[2a(r + a - \gamma) - 2ay^*(r + a - \gamma) + k\mu(r + a) - \gamma(a + d)].$$

To determine the sign of C, we consider the following two cases separately:

(a) $0 < \mu_1 < \mu < \mu_0$. From (4), we have

$$2a(r + a - \gamma)y^* = -\mathcal{B} - \sqrt{\Delta},$$

therefore, $C = \frac{s\mu x^* y^*}{2 - y^*}[\sqrt{\Delta}]$, which is positive.

(b) $0 < \mu_0 < \mu < \mu_1$. In this case,

$$2a(r + a - \gamma)y^* = -\mathcal{B} + \sqrt{\Delta},$$

thus $C = -\frac{s\mu x^* y^*}{2 - y^*}[\sqrt{\Delta}]$, which is negative.

In contrast by substituting $z^* = \mu(1 - ky^*)$ and $\frac{z^*}{2 - y^*} = \gamma - \gamma x^* + (a - \gamma)y^*$ in the expression for $AB - C$, and after some algebraic simplification, we get

$$\begin{aligned} AB - C &= (\gamma x^* + ry^*)(ax^* y^*(a - \gamma + r) + s\mu(\gamma x^* + ry^* + s\mu)) \\ &\quad - \frac{(a + r)x^* y^*(\gamma x^* + ry^* - (a + r)y^*)(\gamma x^* + ry^*)}{2 - y^*} - \frac{(a + r)ks\mu^2 x^* y^*}{2 - y^*} \\ &\geq ax^* y^*(a - \gamma + r)(\gamma x^* + ry^*) + s\mu(\gamma x^* + ry^* + s\mu)[\gamma x^* + ry^* - (a + r)x^* y^*] \\ &= ax^* y^*(a - \gamma + r)(\gamma x^* + ry^*) + s\mu(\gamma x^* + ry^* + s\mu)[x^*(\gamma - ay^*) + ry^*(1 - x^*)] \\ &> 0, \end{aligned}$$

under the assumption (3). By the Routh–Hurwitz criterion, all eigenvalues have negative real parts if and only if $A > 0$, $C > 0$, and $AB - C > 0$.

Therefore, E^* is locally asymptotically stable if $0 < \mu_1 < \mu < \mu_0$ and it is unstable if $0 < \mu_0 < \mu < \mu_1$.

We summarize the above results as follows:

Theorem 1. *Let (3) holds, then the system (2) has one trivial equilibrium O, three axial equilibria R, N, and Q, and two boundary equilibria D and F. Moreover,*

- **(a)** *The trivial equilibrium point O is an unstable node, whereas the axial equilibrium points R, N, and Q are saddle points.*
- **(b)** *The boundary point D is a stable node if* $0 < \mu_0 < \mu$ *and it is a saddle if* $0 < \mu < \mu_0$.
- **(c)** *The boundary point F is a stable node if* $0 < \mu < \mu_1$ *and it is a saddle if* $0 < \mu_1 < \mu$.
- **(d)** *If* $0 < \mu_1 < \mu < \mu_0 (0 < k_0 < k)$, *then there is a unique interior equilibrium* E^*, *which is asymptotically stable.*
- **(e)** *If* $0 < \mu_0 < \mu < \mu_1 (0 < k < k_0 < 1)$, *a unique interior equilibrium* E^* *exists, which is unstable.*

We note that although E^* changes its stability, however it is not possible to have a Hopf bifurcation there. Because for that to happen, it is necessary that Equation (7) has purely imaginary roots $\lambda = \pm i\omega$ and it should be in the following form:

$$\lambda^3 + A\lambda^2 + B\lambda + C = (\lambda^2 + \omega^2)(\lambda + A).$$

It is easy to verify that this holds only if $B = \omega^2$ and $C = A\omega^2$. Because A is always positive, this implies that $C > 0$, $B > 0$, and $AB - C = 0$. However, we prove that under the assumption (3),

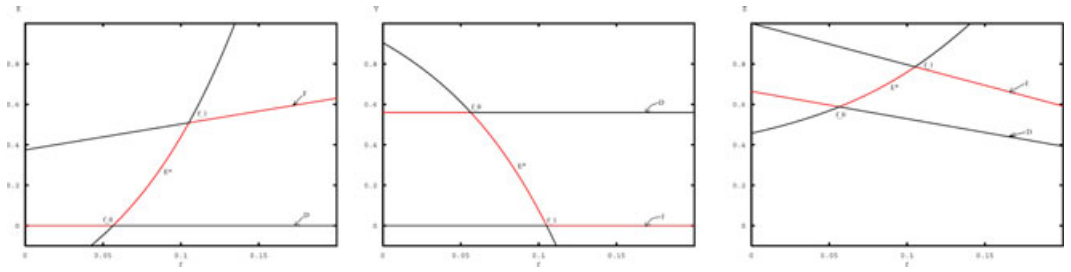

FIGURE 1 One-parameter bifurcation diagrams for the system (2) produced by AUTO, with $k = 0.6$ and f as the bifurcation parameter, showing a transcritical bifurcation of D and E^* at $f_0 = 0.05645$ and a transcritical bifurcation of E^* and F at $f_1 = 0.10512$. Other parameter values are $a = 0.1$, $d = 0.44$, $s = 0.49$, $\gamma = 0.8$, $r = 1$. All panels show f on the horizontal axis, whereas the vertical axes are x, y, and z in the left, middle, and right panels, respectively. Solid red lines correspond to branches of stable equilibria, and solid black lines to unstable equilibria. The portions of branches corresponding to $x < 0$ and $y < 0$ have no significance in the model, but are shown to clarify the transcritical bifurcation and change of stability

$AB - C$ is always positive. Then, Equation (7) cannot have purely imaginary roots. Also, for a set of particular parameter values, we have numerically computed $AB - C$ and used the path continuation AUTO to numerically find the various bifurcations.

For example, when $a = 0.1$, $d = 0.44$, $s = 0.49$, $\gamma = 0.8$, $r = 1$, $k = 0.6$, we obtain $f_0 = 0.05645$ and $f_1 = 0.10512$. This suggests that only the transcritical bifurcation can occur. See Figure 1.

Now, we consider the global behavior of the system (2). Because, in our system, all variables should be nonnegative, we are only interested in the dynamics of model (2) in the closed first octant $\mathbb{R}^3_+$. First, we remind the definition of a uniformly persistent region.

Definition 1 (see Chen, 2005). If there exists a compact set $\mathcal{D} \subseteq \operatorname{Int} \mathbb{R}^3_+ = \Omega$, such that all solutions of (2) with initial condition eventually enter and remain in region $\mathcal{D}$, then the system (2) is called uniformly persistent.

Now, let us denote

$$\mathcal{D} = \{(x, y, z):\ 0 \le x \le 1,\ 0 \le y \le 1,\ 0 \le z \le 1\}. \tag{8}$$

The vector field defined by system (2) is locally Lipschitz continuous in $\mathcal{D}$, which guarantees the existence and uniqueness of their solutions.

In the following, we show that the region $\mathcal{D}$ defined above is uniformly persistent under the flow of (2).

Lemma 1. *The set $\mathcal{D}$ in (8) is an attracting set for the system (2).*

Proof. Consider the system (2). First of all, it is clear that the planes $x = 0$, $y = 0$, and $z = 0$ are invariant under the flow of system (2). Now, we show that all orbits with initial

conditions $(x_0,\ y_0,\ z_0) \in \Omega$ with $1 \le y_0 \le M < 2$ will eventually enter region $\mathcal{D}$. To show this, we note that for $x_0 \ge 1$, we have

$$\dot{x} \le \gamma(1-x)x - (\gamma - a)y < 0.$$

This implies that there is some finite time T_0 such that for $t \ge T_0$, we have $x(t) \le 1$. Similarly, if $y_0 \ge 1$, then

$$\begin{aligned} \dot{y} &\le (r-d) - ry - (r+a)x \\ &= -(d + (r+a)x) \le -d < 0. \end{aligned}$$

Therefore, there is some finite T_1 such that for $t \ge T_1$, we have $y(t) \le 1$. Also, for $z_0 \ge 1$,

$$\dot{z} \le \left[(s-f) - \frac{s}{1-ky}\right] = \left[-f - \frac{sky}{1-ky}\right] < -f.$$

Thus, there is some finite time T_2 so that for $t > T_2$, $z(t) \le 1$. Previous discussion and the invariance of the planes $x = 0,\ y = 0$, and $z = 0$ imply that the cube $\mathcal{D}$ is an attracting set for system (2). □

Theorem 2. *Suppose $0 < \mu_1 < \mu < \mu_0$ and assumption (3) are satisfied, then the region $\mathcal{D}$ defined by Lemma 1 is uniformly persistent under the flow of the system (2).*

Proof. We prove this theorem by the method of average Lyapunov function (cf., Gard & Hallam, 1979; Hutson, 1986). Let $v(x, y, z) = xyz^{\alpha}$, where α is a positive constant to be determined. Therefore,

$$\begin{aligned} \xi(x,y,z) := \frac{\dot{v}}{v} = \frac{\dot{x}}{x} + \frac{\dot{y}}{y} + \alpha\frac{\dot{z}}{z} &= \left[\gamma - \gamma x + (a-\gamma)y - \frac{z}{2-y}\right] \\ &+ [(r-d) - (r+a)x - ry] + \alpha\left[s - f - \frac{sz}{1-ky}\right]. \end{aligned}$$

Now, we consider the value of $\xi(x, y, z)$ at each of the boundary equilibria (limit set of (2) on the boundary of $\mathcal{D}$) and prove that this function is positive at each of these boundary equilibria. We have

$$\begin{aligned} \xi(O) &= \xi(0,0,0) = \gamma + (r-d) + (s-f), \\ \xi(R) &= \xi(0,0,\mu) = \left(\gamma - \tfrac{\mu}{2}\right) + r - d, \\ \xi(N) &= \xi\left(0, \tfrac{r-d}{r}, 0\right) = \left[\tfrac{a(r-d)+\gamma d}{r}\right] + \alpha(s-f), \end{aligned}$$

which are positive by the assumption (3). At the equilibrium $Q = (1, 0, 0)$, we obtain $\xi(1, 0, 0) = -(a + d) + \alpha(s - f)$. For any given set of parameters $a,\ d,\ s$, and f, it is sufficient to choose $\alpha > \frac{a+d}{s-f}$, therefore $\xi(Q)$ is positive. Likewise, we get the values of ξ at equilibria D and F, respectively,

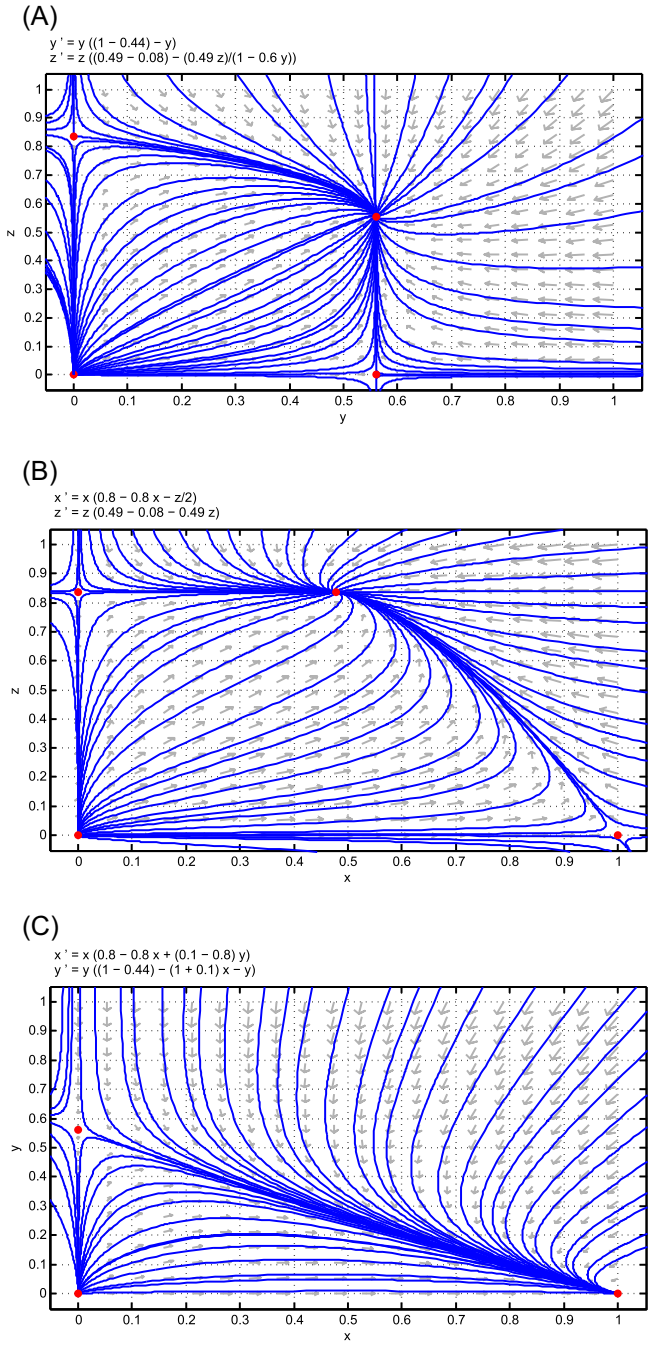

FIGURE 2 (a) Equilibrium covers of coral reef and parrotfish and trajectories over time, (b) equilibrium covers of macroalgae and parrotfish, and (c) the phase portrait of macroalgae and corals

$$\begin{aligned}\xi(D) &= \left[\gamma + (a-\gamma)\frac{r-d}{r} - \mu\frac{r(1-k)+kd}{r+d}\right] \\ &= \frac{r(1-k)+kd}{r+d}\left(\frac{a(r-d)(r+d)+\gamma d(r+d)}{r(r(1-k)+kd)} - \mu\right) \\ &= \frac{r(1-k)+kd}{r+d}(\mu_0 - \mu), \\ \xi(F) &= \left[r - d - (r+a)\left(1 - \frac{\mu}{2\gamma}\right)\right] = \frac{\mu}{2\gamma}(r+a) - (d+a) \\ &= \frac{r+a}{2\gamma}\left(\mu - \frac{2\gamma(a+d)}{r+a}\right) = \frac{r+a}{2\gamma}(\mu - \mu_1),\end{aligned}$$

which are positive. Therefore, ν is an average Lyapunov function and thus, the system (2) is uniformly persistent by Theorem 3.1 in Hutson (1986). □

4 | THE DDE MODEL AND ITS MATHEMATICAL ANALYSIS

In this section, we have all assumptions about the system (2) and hypothesis (3) satisfied and further assume that

$$0 < \mu_1 < \mu < \mu_0, \tag{9}$$

so that there is a unique stable interior equilibrium. It has been suggested by Blackwood and Hastings (2011) that the inherent time delay has significant impact on dynamics of coral–algae interactions. Here, we construct the following delay model by using the fact that it takes a long time before algal turfs accumulate growth after macroalgae are grazed by parrotfish:

$$\begin{cases}\frac{dx}{dt} = x[(a-\gamma)y + \gamma - \gamma x] - \frac{z(t-\tau)x(t-\tau)}{2-y(t-\tau)}, \\ \frac{dy}{dt} = y[r - d - (r+a)x - ry], \\ \frac{dz}{dt} = z\left[(s-f) - \frac{sz}{1-ky}\right].\end{cases} \tag{10}$$

In the following, we are interested in stability of equilibria in the DDE model (10).

4.1 | Stability analysis of equilibria

The equilibrium points of the system (10) are the same as those of the system (2). The linearized system takes the form

$$\begin{pmatrix}\frac{dx}{dt} \\ \frac{dy}{dt} \\ \frac{dz}{dt}\end{pmatrix} = A_1\begin{pmatrix}x(t) \\ y(t) \\ z(t)\end{pmatrix} + A_2\begin{pmatrix}x(t-\tau) \\ y(t-\tau) \\ z(t-\tau)\end{pmatrix},$$

where

$$A_1 = \begin{pmatrix} \gamma - 2x\gamma + (a-\gamma)y & (a-\gamma)x & 0 \\ -(a+r)y & r - d - 2ry - (a+r)x & 0 \\ 0 & \frac{-ksz^2}{(1-ky)^2} & s - f - \frac{2sz}{1-ky} \end{pmatrix}, \tag{11}$$

$$A_2 = \begin{pmatrix} \frac{-z(t)}{2-y(t)} & -\frac{z(t)x(t)}{(2-y(t))^2} & -\frac{x(t)}{2-y(t)} \\ 0 & 0 & 0 \\ 0 & 0 & 0 \end{pmatrix}. \tag{12}$$

Now, we analyze the stability of these equilibria. At the equilibrium $O = (0, 0, 0)$, we have $A_1 = J(O)$ and $A_2 = [0]_{3\times 3}$, then the equilibrium O remains unstable for any value of the delay τ.

At the equilibrium $R = \left(0, 0, \frac{s-f}{s}\right)$, we have A_1 and A_2 as

$$A_1 = \begin{pmatrix} \gamma & 0 & 0 \\ 0 & r-d & 0 \\ 0 & -ks\mu^2 & -s\mu \end{pmatrix}, \quad A_2 = \begin{pmatrix} -\frac{\mu}{2} & 0 & 0 \\ 0 & 0 & 0 \\ 0 & 0 & 0 \end{pmatrix}.$$

Then, the characteristic equation is given by

$$\det\left(\lambda I - A_1 - A_2 e^{-\lambda\tau}\right) = \left(\lambda - \gamma - \frac{\mu}{2}e^{-\lambda\tau}\right)(\lambda - r + d)(\lambda + s\mu). \tag{13}$$

For $\tau = 0$, the eigenvalues are $\lambda_1 = \gamma - \frac{\mu}{2} > 0$, $\lambda_2 = r - d > 0$, and $\lambda_3 = -s\mu < 0$. Thus, the axial equilibrium R is unstable. For $\tau > 0$, as the time delay τ increases, any changes in the sign of real part of eigenvalues correspond to a purely imaginary root $\lambda = i\omega$. Now, we assume that there is some $\tau^* = \tau > 0$ such that Equation (13) has a root $\lambda(\tau) = \alpha(\tau) + i\omega(\tau)$ satisfying $\alpha(\tau^*) = 0$, $\lambda(\tau^*) = i\omega(\tau^*) = i\omega$. Then,

$$i\omega = \gamma - \frac{\mu}{2}e^{-i\omega\tau^*} = \gamma - \frac{\mu}{2}\cos\,\omega\tau^* + i\frac{\mu}{2}\sin\,\omega\tau^*. \tag{14}$$

By equating the real and imaginary parts of (14) and using the identity $\sin^2\,\omega\tau^* + \cos^2\,\omega\tau^* = 1$, we obtain

$$\omega^2 = \frac{\mu^2 - 4\gamma^2}{4} = \frac{1}{4}(\mu - 2\gamma)(\mu + 2\gamma),$$

which is negative due to $\mu < 2\gamma$ in the assumption (3). Therefore, Equation (13) has no purely imaginary roots, and hence, the number of roots with positive real parts of Equation (13) does not change as the time delay τ increases (cf., Cooke & Grossman, 1982). Therefore, for any $\tau > 0$, the linearized equation of the system (10) at the equilibrium R has one negative eigenvalue, two positive eigenvalues, and all other eigenvalues have negative real parts. Consequently, for any $\tau > 0$, the axial equilibrium R is unstable.

By similar argument, we can conclude that the time delay has no effect on the stability of the equilibria $N = (0, \frac{r-d}{r}, 0)$ and $Q = (1, 0, 0)$. We omit the details here.

Now, we discuss the stability of the equilibrium $D = (0, \frac{r-d}{r}, \frac{\mu(r(1-k)+kd)}{r})$. At this equilibrium, A_1 and A_2 are

$$A_1 = \begin{pmatrix} \gamma + (a-\gamma)\left(\frac{r-d}{r}\right) & 0 & 0 \\ -(a+r)\left(\frac{r-d}{r}\right) & -(r-d) & 0 \\ 0 & -ks\mu^2 & -s\mu \end{pmatrix}, \quad A_2 = \begin{pmatrix} \frac{-\mu(r(1-k)+kd)}{(r+d)} & 0 & 0 \\ 0 & 0 & 0 \\ 0 & 0 & 0 \end{pmatrix}.$$

Then, the characteristic equation is

$$\left[\lambda - \gamma - (a-\gamma)\left(\frac{r-d}{r}\right) + \frac{(s-f)(r(1-k)+kd)}{s(r+d)}e^{-\lambda\tau}\right][\lambda + (r-d)][\lambda + s\mu] = 0.$$

Hence, two of the eigenvalues are $\lambda_2 = -(r-d)$ and $\lambda_3 = -s\mu$, which are negative [under the assumption (3)]. The other eigenvalue satisfies

$$\begin{aligned} \lambda &= \gamma + (a-\gamma)\left(\frac{r-d}{r}\right) - \frac{\mu(r(1-k)+kd)}{(r+d)}e^{-\lambda\tau} \\ &= \frac{r(1-k)+kd}{(r+d)}[\mu_0 - \mu e^{-\lambda\tau}]. \end{aligned} \tag{15}$$

Recall that for $\tau = 0$, the eigenvalues are $\lambda_1 = \frac{r(1-k)+kd}{(r+d)}(\mu_0 - \mu)$, $\lambda_2 = -(r-d) < 0$, and $\lambda_3 = -s\mu < 0$. Thus, D is a saddle point. For $\tau > 0$, we assume that there exists $\tau^* = \tau > 0$, then Equation (15) has a complex root $\lambda(\tau) = \alpha(\tau) + i\omega(\tau)$ satisfying $\alpha(\tau^*) = 0$, $\lambda(\tau^*) = i\omega(\tau^*) = i\omega$. Then,

$$i\omega = \frac{r(1-k)+kd}{(r+d)}[(\mu_0 - \mu\cos\omega\tau^*) + i\mu\sin\omega\tau^*]. \tag{16}$$

Therefore, by equating the real and imaginary parts of (16), we obtain

$$\omega^2 = \frac{(r(1-k)+kd)^2}{(r+d)^2}(\mu^2 - \mu_0^2) < 0.$$

Again there are no purely imaginary roots for Equation (15). Thus, the number of roots with positive real parts of Equation (15) does not change as the time delay τ increases (cf., Cooke & Grossman, 1982). Therefore, for any $\tau > 0$, the linearized equation of the system (10) at the equilibrium D has one positive eigenvalue, two negative eigenvalues, and all other eigenvalues have negative real parts. Therefore, the boundary equilibrium D is unstable for any $\tau > 0$.

At the equilibrium $F = (1 - \frac{\mu}{2\gamma}, 0, \mu)$, A_1 and A_2 take the form

$$A_1 = \begin{pmatrix} -\gamma+\mu & (a-\gamma)\left(1-\frac{\mu}{2\gamma}\right) & 0 \\ 0 & -a-d+(a+r)\frac{\mu}{2\gamma} & 0 \\ 0 & -ks(\mu)^2 & -s\mu \end{pmatrix},$$

$$A_2 = \begin{pmatrix} \frac{-\mu}{2} & -\frac{\mu}{2}\left(1-\frac{\mu}{2\gamma}\right) & -\frac{1}{2}\left(1-\frac{\mu}{2\gamma}\right) \\ 0 & 0 & 0 \\ 0 & 0 & 0 \end{pmatrix}.$$

It can be easily verified that two of the eigenvalues are

$$\lambda_2 = -\frac{(r+a)}{2\gamma}(\mu-\mu_1), \quad \lambda_3 = -s\mu,$$

and the third eigenvalue satisfies

$$\lambda = -\gamma+\mu-\left(\frac{\mu}{2}\right)e^{-\lambda\tau}. \tag{17}$$

Recall that for $\tau=0$, the eigenvalues are $\lambda_1 = -\gamma+\frac{\mu}{2}<0$, $\lambda_2 = \frac{(r+a)}{2\gamma}(\mu-\mu_1)>0$, and $\lambda_3 = -s\mu<0$. For $\tau>0$, we assume that $\lambda(\tau)=\alpha(\tau)+i\omega(\tau)$ is a root of Equation (17) satisfying $\alpha(\tau^*)=0$, $\lambda(\tau^*)=i\omega(\tau^*)=i\omega$ for some $\tau^*>0$. Then,

$$i\omega = -\gamma+\mu-\left(\frac{\mu}{2}\right)e^{-i\omega\tau^*} = -\gamma+\mu-\left(\frac{\mu}{2}\right)\cos\,\omega\tau^* + i\left(\frac{\mu}{2}\right)\sin\,\omega\tau^*. \tag{18}$$

Therefore, we obtain

$$\omega^2 = \frac{1}{4}[(2\gamma-\mu)(3\mu-2\gamma)]. \tag{19}$$

Thus, for $\mu<\frac{2\gamma}{3}$, Equation (17) has no purely imaginary roots, but for $\mu_1<\frac{2\gamma}{3}<\mu<2\gamma$, there is a sequence of time delays $\tau_0^+<\tau_1^-<\cdots<\tau_j^+<\tau_{j+1}^-<\cdots$, with

$$\tau=\tau_j^{\pm}=\frac{1}{\omega}\left\{\pm\arccos\left(2\left(1-\frac{\gamma}{\mu}\right)\right)+2\pi j\right\}, \quad j=0,\,1,\,2,\ldots,$$

where Equation (17) has a pair of purely imaginary roots $\lambda=\pm i\omega$ with

$$\omega=\frac{1}{2}\sqrt{(2\gamma-\mu)(3\mu-2\gamma)}. \tag{20}$$

Now, we compute $\frac{d\tau}{d\lambda}=(\frac{d\lambda}{d\tau})^{-1}$ from (17) and obtain $(\frac{d\lambda}{d\tau})^{-1}=\frac{2e^{\lambda\tau}}{\lambda\mu}-\frac{\tau}{\lambda}$. Therefore,

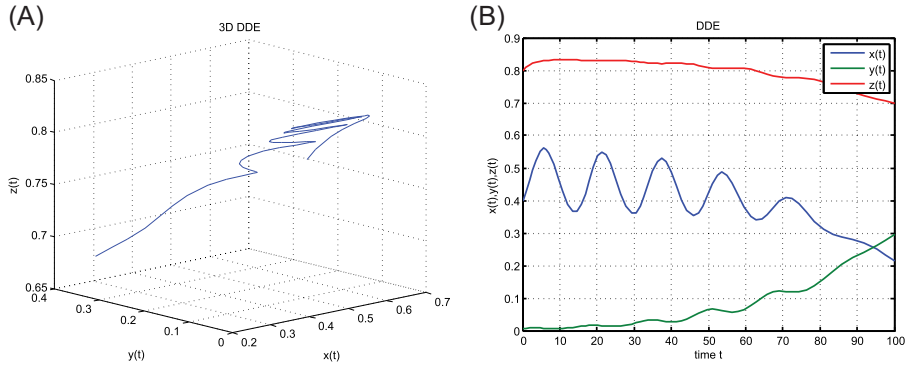

FIGURE 3 (a,b) Solution of the system (10), with initial condition (0.4, 0.007, 0.8) and time delay $\tau = 3.55$. DDE: delay differential equation; 3D: three dimensional

$$\mathrm{Re}\left(\frac{d\lambda}{d\tau}\right)^{-1}|_{\lambda=\pm i\omega} = \frac{d\,\mathrm{Re}\,\tau}{d\lambda}|_{\lambda=\pm i\omega} = \frac{2\sin\omega\tau}{\mu\omega} = \frac{4}{\mu^2} > 0,$$

which implies that $(\frac{d\,\mathrm{Re}\,\lambda(\tau)}{d\tau})|_{\tau=\tau_j^{\pm}}$ is positive for $j = 0, 1, 2,\ldots$. Therefore, for $0 < \tau < \tau_0^+$, the linearized equation at the equilibrium F has one negative eigenvalue, one positive eigenvalue, and all the others have negative real parts. Thus, the equilibrium F is unstable. When $\tau = \tau_j^{\pm}$ $(j = 1, 2,\ldots)$, the characteristic equation (17) has a pair of purely imaginary roots. For every j, as the time delay τ increases and passes through $\tau = \tau_j^{\pm}$, the number of eigenvalues with positive real parts increases by two. Therefore, for $\tau > \tau_0^+$, trajectories about F are oscillatory and move away from F (see Figure 3). We summarize the above discussions in the following theorem.

Theorem 3. *Consider the system (10) and assume that hypotheses (3) and (9) are satisfied. Then,*

- **(a)** *For all $\tau > 0$, the characteristic equation about the trivial solution O, axial solutions R, N, and Q, and the boundary point D will have no pure imaginary eigenvalues and delay has no effect on their stability.*
- **(b)** *If $\mu_1 < \mu < \frac{2\gamma}{3}$, then the characteristic equation about F will have no pure imaginary eigenvalues and delay has no effect on their stability. However, for $\mu > \frac{2\gamma}{3} > \mu_1$, there will be a sequence of time delays $\tau = \tau_j^{\pm}$, $j = 1, 2,\ldots$ so that as the time delay τ increases and passes through $\tau = \tau_j^{\pm}$, the number of eigenvalues with positive real parts increases by two.*

Now, we investigate the dynamics of the delay system (10) about the interior equilibrium $E^* = (x^*, y^*, z^*)$. We have already proved that under the condition (9), this point is asymptotically stable for $\tau = 0$. For, $\tau > 0$, A_1 and A_2 have the following form, respectively,

$$A_1 = \begin{pmatrix} \gamma - 2x^*\gamma + (a-\gamma)y^* & (a-\gamma)x^* & 0 \\ -(a+r)y^* & -ry^* & 0 \\ 0 & -ks\mu^2 & -s\mu \end{pmatrix},$$

$$A_2 = \begin{pmatrix} \frac{-z^*}{2-y^*} & -\frac{z^*x^*}{(2-y^*)^2} & -\frac{x^*}{2-y^*} \\ 0 & 0 & 0 \\ 0 & 0 & 0 \end{pmatrix}.$$

Then, the characteristic equation is given by

$$\lambda^3 + \lambda^2(a_1 + a_2 e^{-\lambda\tau}) + \lambda(a_3 + a_4 e^{-\lambda\tau}) + (a_5 + a_6 e^{-\lambda\tau}) = 0, \tag{21}$$

where

$$\begin{aligned} a_1 &:= -\gamma + 2x^*\gamma - (a-\gamma)y^* + s\mu + ry^*, \\ a_2 &:= \frac{z^*}{2-y^*} = \gamma - \gamma x^* + (a-\gamma)y^*, \\ a_3 &:= (s\mu + ry^*)(-\gamma + 2x^*\gamma - (a-\gamma)y^*) + ry^*s\mu + (a+r)(a-\gamma)x^*y^*, \\ a_4 &:= \frac{z^*}{2-y^*}(s\mu + ry^*) - \frac{(a+r)x^*y^*z^*}{(2-y^*)^2}, \\ a_5 &:= rs\mu y^*(-\gamma + 2x^*\gamma - (a-\gamma)y^*) + (a+r)s\mu(a-\gamma)x^*y^*, \\ a_6 &:= rs\mu\frac{z^*y^*}{2-y^*} + \frac{kx^*y^*(a+r)s\mu^2}{(2-y^*)} - \frac{(a+r)s\mu x^*y^*z^*}{(2-y^*)^2}. \end{aligned}$$

When $\tau = 0$, the characteristic equation (21) is given by

$$\lambda^3 + (a_1 + a_2)\lambda^2 + (a_3 + a_4)\lambda + (a_5 + a_6) = 0. \tag{22}$$

By comparing with Equation (7) and according to the conclusion in Section 2, we have $A \equiv (a_1 + a_2) > 0$, $B \equiv (c_3 + c_4) > 0$, and $C \equiv (a_5 + a_6) > 0$, and all three eigenvalues are negative. When $\tau > 0$, let $\lambda(\tau) = \alpha(\tau) + i\omega(\tau)$ be a root of Equation (21) satisfying $\alpha(\tau^*) = 0$, $\lambda(\tau^*) = i\omega(\tau^*) = i\omega$ for some $\tau^* > 0$. If $\lambda = i\omega$ is a root, then $\omega \neq 0$ and

$$-i\omega^3 - a_1\omega^2 - a_2\omega^2 e^{-i\omega\tau^*} + a_3 i\omega + a_4 i\omega e^{-i\omega\tau^*} + a_5 + a_6 e^{-i\omega\tau^*} = 0. \tag{23}$$

By equating the real and imaginary parts of (23) equal to zero, we have

$$\begin{cases} -\omega^3 + a_3\omega + (a_2\omega^2 - a_6)\sin\omega\tau^* + a_4\omega\cos\omega\tau^* = 0, \\ -a_1\omega^2 + a_5 + a_4\omega\sin\omega\tau^* - (a_2\omega^2 - a_6)\cos\omega\tau^* = 0. \end{cases} \tag{24}$$

It follows from (24) that

$$\omega^6 + \left(a_1^2 - 2a_3 - a_2^2\right)\omega^4 + \left(a_3^2 - 2a_1a_5 - a_4^2 + 2a_2a_6\right)\omega^2 + a_5^2 - a_6^2 = 0. \tag{25}$$

Denote

$$A_1 := \left(a_1^2 - 2a_3 - a_2^2\right), \quad B_1 := \left(a_3^2 - 2a_1a_5 - a_4^2 + 2a_2a_6\right), \quad C_1 := a_5^2 - a_6^2,$$

and let $\omega^2 := \zeta$, then Equation (25) becomes

$$h(\zeta) := \zeta^3 + A_1\zeta^2 + B_1\zeta + C_1 = 0. \tag{26}$$

The cubic function $h(\zeta)$ can have at most three positive roots, which are denoted by $\zeta_i = \omega_i^2$, $i = 1, 2, 3$ with $0 < \omega_1 < \omega_2 < \omega_3$. Also, from (24), we get

$$\cos\,\omega\tau^* = \frac{(a_4 - a_1a_2)\omega^4 + (a_1a_6 - a_4a_3 + a_2a_5)\omega^2 - a_5a_6}{a_4^2\omega^2 + (a_2\omega^2 - a_6)^2},$$
$$\sin\,\omega\tau^* = \frac{a_2\omega^5 + (-a_6 + a_4a_1 - a_2a_3)\omega^3 + (a_3a_6 - a_5a_4)\omega}{a_4^2\omega^2 + (a_6 - a_2\omega^2)^2}.$$

Then, corresponding to each positive root ζ_i, $i = 1, 2, 3$ of $h(\zeta)$, there exist a sequence of time delays $0 < \tau_{i,0}^+ < \tau_{i,1}^- < \cdots < \tau_{i,n}^+ < \tau_{i,n+1}^- < \cdots$ such that (22) has a pair of pure imaginary eigenvalues, where

$$\tau_{i,n}^{\pm} = \frac{1}{\omega_i}\left[\pm\arccos\left\{\frac{(a_4 - a_1a_2)\omega_i^4 + (a_1a_6 - a_4a_3 + a_2a_5)\omega_i^2 - a_5a_6}{a_4^2\omega_i^2 + (a_2\omega_i^2 - a_6)^2}\right\} + 2n\pi\right], \tag{27}$$

for $i = 1, 2, 3$, $n = 0, 1, 2,....$

Now, we discuss the stability of the interior equilibrium E^* according to the number of positive roots for Equation (25). There are four cases of interest:

(I) Equation (25) has no positive roots. Then, delay has no effect on the stability of E^*, which is asymptotically stable for all $\tau > 0$.

(II) $h(\zeta)$ only has one simple positive root $\zeta_1 = \omega_1^2$. There is one positive root for Equation (25), which is simple. Thus, for $\tau = \tau_{1,n}^{\pm}$, the characteristic equation (21) has a pair of purely imaginary roots. To discuss the possible Hopf bifurcation about E^* as τ passes through $\tau_{1,n}^{\pm}$, we need to determine $\text{sign}\{\frac{d(\text{Re}\,\lambda)}{d\tau}\}_{\tau=\tau_{1,n}^{\pm}}$. From Equation (21), we have

$$\left(\frac{d\lambda}{d\tau}\right)^{-1} = \frac{e^{\lambda\tau}(3\lambda^2 + 2a_1\lambda + a_3) + 2a_2\lambda + a_4}{(a_2\lambda^2 + a_4\lambda + a_6)\lambda} - \frac{\tau}{\lambda}, \quad e^{\lambda\tau} = \frac{-(a_2\lambda^2 + a_4\lambda + a_6)}{\lambda^3 + a_1\lambda^2 + a_3\lambda + a_5}.$$

Thus,

$$\begin{aligned}
&\operatorname{sign}\left\{\frac{d(\operatorname{Re}\lambda)}{d\tau}\right\}_{\tau=\tau_{1,n}^{\pm}} = \operatorname{sign}\left\{\operatorname{Re}\left(\frac{d\lambda}{d\tau}\right)^{-1}\right\}_{\lambda=i\omega_1}\\
&= \operatorname{sign}\left\{\operatorname{Re}\left[\frac{-(3\lambda^2+2a_1\lambda+a_3)}{\lambda(\lambda^3+a_1\lambda^2+a_3\lambda+a_5)} + \frac{2a_2\lambda+a_4}{\lambda(a_2\lambda^2+a_4\lambda+a_6)}\right]_{\lambda=i\omega_1}\right\}\\
&= \operatorname{sign}\left\{\frac{(\zeta_1-a_3)(3\zeta_1-a_3)+2a_1(a_1\zeta_1-a_5)}{\zeta_1(\zeta_1-a_3)^2+(a_1\zeta_1-a_5)^2} - \frac{a_4^2+2a_2(a_2\zeta_1-a_6)}{a_4^2\zeta_1+(a_2\zeta_1-a_6)^2}\right\}\\
&= \operatorname{sign}\left\{\frac{3\zeta_1^2+2\left(a_1^2-2a_3-a_2^2\right)\zeta_1+\left(a_3^2-2a_1a_5-a_4^2+2a_2a_6\right)}{(a_2\zeta_1-a_6)^2+a_4^2\zeta_1}\right\}\\
&= \operatorname{sign}\{h'(\zeta_1)\} > 0,
\end{aligned}$$

because $(a_2\zeta_1 - a_6)^2 + a_4^2\zeta_1 > 0$. Characteristic equation (21) with $\tau = 0$ has three negative eigenvalues, then when $0 < \tau < \tau_{1,0}^{+}$, the characteristic equation (21) has the eigenvalues with negative real parts, and thus the equilibrium E^* is asymptotically stable. When $\tau = \tau_{1,0}^{+}$, the characteristic equation (21) has a pair of purely imaginary roots $\pm i\omega_1$ and $h'(\zeta_1) > 0$, then as τ increase through $\tau_{1,n}^{\pm}$, a Hopf bifurcation occurs, and a nontrivial periodic solution appears. When $\tau_{1,0}^{+} < \tau < \tau_{1,1}^{-}$, the characteristic equation (21) has a pair of eigenvalues with positive real parts, whereas the others with negative real parts, hence the equilibrium E^* becomes unstable, and so on. Therefore, after a pair of imaginary eigenvalues appear, the stability of the solution can only be lost but not regained as τ increases.

(III) If Equation (25) has a pair of positive roots with double multiplicity $\omega_1^2 = \zeta_1$, then $h'(\zeta_1) = 0$, then the transversality condition for the Hopf bifurcation does not hold, thus the direction of movement of eigenvalues by increasing τ depends on the higher derivatives, which are very complex. Now, suppose there are two positive simple roots $\omega_1 = \sqrt{\zeta_1}$, $\omega_2 = \sqrt{\zeta_2}$ for Equation (25), with $|\omega_2| > |\omega_1|$. In this case, using Equation (24), there are the two sets of values of $\tau = \tau_{i,n}^{\pm}$, $n = 0, 1,\ldots, i = 1, 2$, for which Equation (22) has two pairs of pure imaginary eigenvalues. In this case, $h'(\zeta_1) < 0$ and $h'(\zeta_2) > 0$ and by similar calculation as Case (II), we have

$$\operatorname{sign}\left\{\operatorname{Re}\left(\frac{d\lambda}{d\tau}\right)^{-1}\right\}_{\lambda=i\omega_1} < 0, \quad \operatorname{sign}\left\{\operatorname{Re}\left(\frac{d\lambda}{d\tau}\right)^{-1}\right\}_{\lambda=i\omega_2} > 0.$$

Characteristic equation (21) with $\tau = 0$ has three negative eigenvalues, and $\tau_{2,0}^{+} < \tau_{1,0}^{+}$. Otherwise suppose $\tau_{2,0}^{+} > \tau_{1,0}^{+}$, but $h'(\zeta_1) < 0$, then we should have a pair of complex eigenvalues with positive real parts for $\zeta < \zeta_1$, which is impossible, because $\zeta = \zeta_1$ is the smallest positive value, for which $h(\zeta) = 0$ has a pair of pure imaginary roots. Then, when $0 < \tau < \tau_{2,0}^{+}$, the characteristic equation (21) has three eigenvalues with negative real parts, and thus the equilibrium E^* is asymptotically stable; when $\tau = \tau_{2,0}^{+}$, the characteristic equation (21) has a pair of purely imaginary roots $\pm i\omega_2$, and sign $h'(\zeta_2)$ is positive, then a supercritical Hopf bifurcation occurs, and a nontrivial periodic solution exists for $\tau_{2,0}^{+} < \tau < \tau_{1,0}^{+}$. For these values of τ, the characteristic equation (21) has a pair of eigenvalues with positive real parts, and the others have negative real parts, hence the equilibrium E^* is unstable; when $\tau = \tau_{1,0}^{+}$, the characteristic equation (21) will have another pair of purely imaginary roots $\pm i\omega_1$, and $h'(\zeta_1) < 0$, hence a subcritical Hopf

bifurcation occurs as τ decreases through $\tau_{1,0}^{+}$, and a nontrivial periodic solution bifurcates from the equilibrium E^*; when $\tau_{1,0}^{+} < \tau < \tau_{2,1}^{-}$, the characteristic equation (21) has three eigenvalues with negative real parts, then the equilibrium E^* is asymptotically stable; when $\tau = \tau_{2,1}^{-}$, the characteristic equation (21) has a pair of purely imaginary roots $\pm i\omega_2$, and $h'(\zeta_2) > 0$, then a supercritical Hopf bifurcation occurs, and a nontrivial periodic solution appears as τ increases through for $\tau = \tau_{2,1}^{-}$, and so on. Note that $h'(\zeta_2) > 0$ and $h'(\zeta_1) < 0$, then after one cycle, the number of eigenvalues with positive real parts does not change. Therefore, if there are two imaginary roots, then the stability of the solution can change for a finite number of times as τ increases, and eventually it becomes unstable.

(IV) There are three positive roots

$$\omega_1 = \sqrt{\zeta_1},\ \omega_2 = \sqrt{\zeta_2},\ \omega_3 = \sqrt{\zeta_3}$$

for Equation (25), with $|\omega_3| > |\omega_2| > |\omega_1|$. In this case, using Equation (24), corresponding to each pair of pure imaginary eigenvalues ω_i, $i = 1, 2, 3$, there are two sequences of time delays $\tau = \tau_{i,n}^{\pm}$, $n = 0, 1,..., i = 1, 2, 3$. In this case, $h'(\zeta_1) > 0$, $h'(\zeta_2) < 0$, and $h'(\zeta_3) > 0$, and similar to Case (II), we have

$$\operatorname{sign}\left\{\operatorname{Re}\left(\frac{d\lambda}{d\tau}\right)\right\}_{\tau=\tau_{i,n}^{\pm}} = \operatorname{sign}\{h'(\zeta_i)\}.$$

We know that characteristic equation (21) with $\tau = 0$ has three negative eigenvalues. With similar reasoning as Case (III), the following two cases are possible:

(a) $\tau_{3,0}^{+} < \tau_{2,0}^{+} < \tau_{1,0}^{+}$: When $0 < \tau < \tau_{3,0}^{+}$, the characteristic equation (21) has the eigenvalues with negative real parts, thus the equilibrium E^* is stable; when $\tau = \tau_{3,0}^{+}$, the characteristic equation (21) has a pair of purely imaginary roots $\pm i\omega_3$, and $h'(\zeta_3)$ is positive, then the Hopf bifurcation occurs, and a nontrivial periodic solution exists for $\tau = \tau_{3,0}^{+}$; when $\tau_{3,0}^{+} < \tau < \tau_{2,0}^{+}$, the characteristic equation (21) has a pair of eigenvalues with positive real parts, the others with negative real parts, hence the equilibrium E^* is unstable; when $\tau = \tau_{2,0}^{+}$, the characteristic equation (21) has a pair of purely imaginary roots $\pm i\omega_2$, and $h'(\zeta_2)$ is negative, hence the Hopf bifurcation occurs, and a nontrivial periodic solution bifurcates from E^*; when $\tau_{2,0}^{+} < \tau < \tau_{1,0}^{+}$, the characteristic equation (21) has the eigenvalues with negative real parts, then the equilibrium E^* is stable; when $\tau = \tau_{1,0}^{+}$, the characteristic equation (21) has a pair of purely imaginary roots $\pm i\omega_1$, and $h'(\zeta_1)$ is positive, then the Hopf bifurcation occurs, and a nontrivial periodic solution appears.

(b) $\tau_{1,0}^{+} < \tau_{2,0}^{+} < \tau_{3,0}^{+}$: When $0 < \tau < \tau_{1,0}^{+}$, we can have similar arguments as Case (a) by exchanging indices 1 and 3.

Note that the number of pure imaginary roots of the characteristic equation (21) depends on the sign of C_1 in Equation (26). If C_1 is positive, then one of the two cases (I) or (III) can occur; if C_1 is negative, then one of the two cases (II) or (IV) can occur. We summarize the above discussions in the following theorem.

TABLE 1 Parameter values and definitions

Parameter	Value	Definition
a	0.1	Rate macroalgae directly overgrow coral (1/year)
γ	0.8	Rate macroalgae spread vegetatively over algal turfs (1/year)
r	1	Rate of coral recruitment to algal turfs (1/year)
d	0.44	Natural coral mortality accounts for 2–4% (1/year), and predation accounts for 30% (1/year)
s	0.49	Rate of parrotfish growth (1/year)
k	0.6	Dimensionless parameter that determines the strength of the linear relationship between coral cover and carrying capacity
f	0.08	Rate of destruction of parrotfish resulting from fishing effort

Theorem 4. *Suppose* $\omega_j^2 := \zeta_j$ *and* $h'(\zeta_j) \neq 0$ *for* $j = 1, 2, 3$, *then* $\operatorname{sign} h'(\zeta_j) = \operatorname{sign} \frac{d\lambda(\tau_{j,n}^{\pm})}{d\tau}$, *for* $j = 1, 2, 3$ *and* $n = 0, 1, 2,...$
Moreover, if Equation (26) has one simple positive root ζ_1 *or has two positive roots,* ζ_1, ζ_2 *with* $\zeta_2 < \zeta_1$, *then there is a Hopf bifurcation for the system (10) as* τ *passes through* $\tau_{1,n}^{+}$, *leading to a stable periodic solution that bifurcates from* E^*. *If there are three positive roots of (26),* $\zeta_1 < \zeta_2 < \zeta_3$, *respectively, then*

$$\frac{d\lambda(\tau_{1,n}^{\pm})}{d\tau} > 0, \quad \frac{d\lambda(\tau_{2,n}^{\pm})}{d\tau} < 0, \quad \frac{d\lambda(\tau_{3,n}^{\pm})}{d\tau} > 0, \quad n = 0, 1, 2,...,$$

which implies that there is a Hopf bifurcation as τ *increases through* $\min\{\tau_{1,0}^{+}, \tau_{3,0}^{+}\}$, *leading to a stable periodic orbit.*

5 | NUMERICAL SIMULATIONS

In this section, we carry out some simulations with the following parameters:

$$a = 0.1, \quad d = 0.44, \quad s = 0.49, \quad \gamma = 0.8, \quad r = 1, \quad f = 0.08, \quad k = 0.6, \tag{28}$$

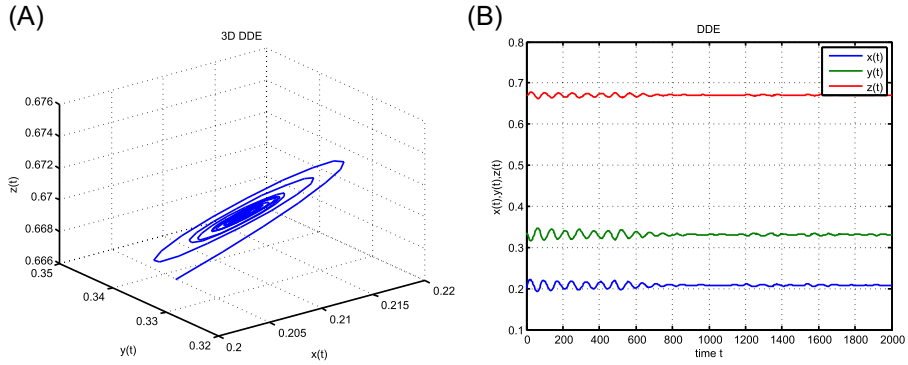

FIGURE 4 (a,b) Solution of the system (10), with initial condition (0.2, 0.33, 0.67) and time delay $\tau = 3.15$ about the equilibrium E^*. DDE: delay differential equation; 3D: three dimensional

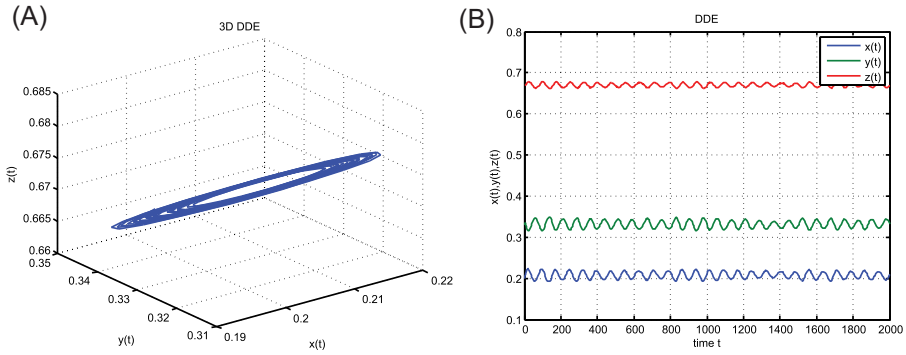

FIGURE 5 (a,b) Solution of the system (10), with initial condition (0.2, 0.33, 0.67) and time delay $\tau = 3.17$ around the equilibrium E^*. DDE: delay differential equation; 3D: three dimensional

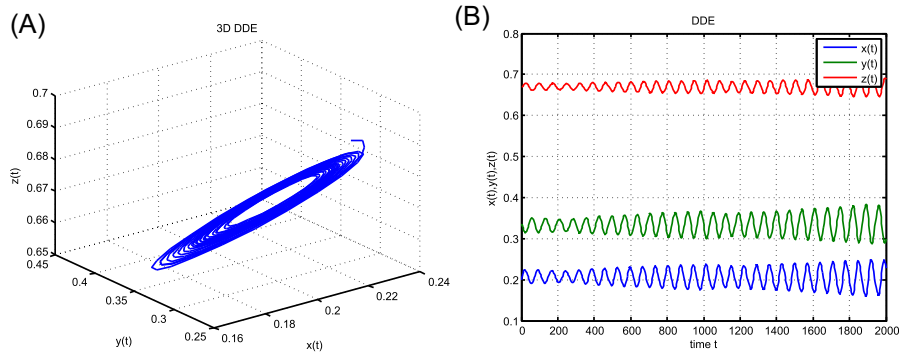

FIGURE 6 (a,b) Solution of the system (10), with initial condition (0.2, 0.33, 0.67) and time delay $\tau = 3.20$ around the equilibrium E^*. DDE: delay differential equation; 3D: three dimensional

where we have a unique stable interior equilibrium E^*. See Table 1 for parameter values and their definitions (these parameter values can be found in Mumby et al., 2007; Mumby, Foster, & Glynn Fahy, 2005). For these values of parameters, the steady states are as follows: $O = (0, 0, 0)$, $R = (0, 0, 0.83673)$, $N = (0, 0.56, 0)$, $Q = (1, 0, 0)$, $D = (0, 0.56, 0.55559)$, $F = (0.47705, 0, 0.83673)$,$E^* = (0.20799, 0.33121, 0.67045)$, and the critical parameter values are $f_0 = 0.05645$, $f_1 = 0.10512$, and $k_0 = 0.45$.

In our analytical study, we know that the boundary planes $\{x = 0\}$, $\{y = 0\}$, and $\{z = 0\}$ are invariant. Hence, the phase portraits of the system (2), in the absence of macroalgae (x), coral reef (y), and parrotfish (z), are given in Figure 2a–c, respectively. As we have seen in our analytical analysis, the boundary point F and the unique interior steady state E^* are the most important equilibrium points from the ecological point of view. Hence, we put emphasis on these in our numerical study. Now, we consider the steady state F. According to Theorem 1, if $f_1 < f < s$, the boundary equilibrium F is stable, but it is unstable for $f < f_1$. Therefore, for the set of parameter values given in (28), F is unstable. Now, we consider the effect of delay, by Theorem 3, we know that if $0 \leq f < f_1 = 0.10512 < f_2 = 0.22867$, the equilibrium F is unstable for all $\tau \geq 0$. Also, when $\tau = \tau_0 = 3.5582$, then Equation (17) has a pair of purely imaginary

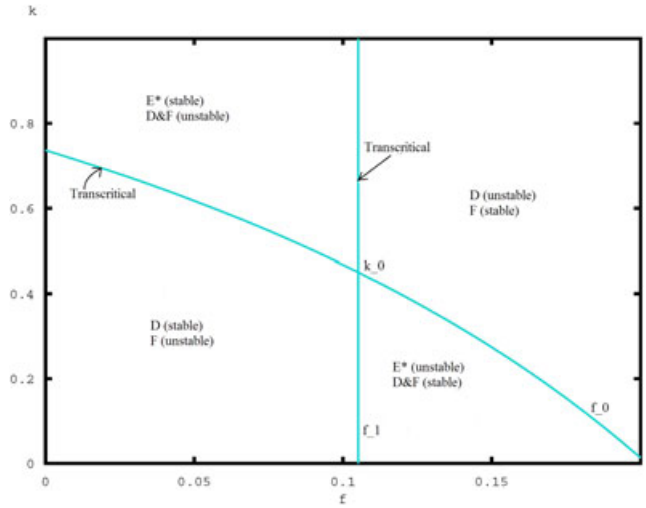

FIGURE 7 Two-parameter bifurcation diagram of the system (2) showing curves of codimension one local bifurcation in the (f, k) parameter plane. Also, regions in (f, k) parameter space, where (2) has positive internal equilibria, for fixed parameter values $a = 0.1$, $d = 0.44$, $s = 0.49$, $\gamma = 0.8$, $r = 1$ have been shown

roots $\lambda = \pm i\omega$ with $\omega = 0.41675$. Trajectories about F are oscillating away from F toward E^* and then away from E^*. This is shown in Figure 3.

By substituting the parameter values in (28) and (7), we obtain

$$A = 0.90760, \quad B = 0.18784, \quad C = 0.002713.$$

Then, by Theorem 1, the equilibrium E^* is stable. Now, we consider the system (10). Case II occurs for the interior equilibrium E^*. Then, as we can see from Figures 4, 5, and 6, the trajectories about E^* change as follows when τ increases:

- **(i)** First, it becomes oscillatory but eventually approaches E^* (due to the appearance of a pair of complex eigenvalues with negative real parts). See Figure 4 as an illustration.
- **(ii)** By increasing the delay τ further, as τ passes through $\tau^+_{1,0}$, a Hopf bifurcation occurs and a stable periodic orbit bifurcates from E^*. See Figure 5 as an illustration.
- **(iii)** By increasing τ further, as τ passes through $\tau^+_{1,1}$, the periodic orbit becomes unstable. See Figure 6 as an illustration.

6 | DISCUSSION

In this paper, we have provided local and global stability analyses of all steady states of the coral reef ODE model (2) under fishing. We have proved that there is an ecologically meaningful attracting region, for which the system is uniformly persistent. We have shown that fishing plays a crucial role on the coral reef dynamics. If the fishing rate is lower than some threshold ($f < f_0$), the coral–parrotfish state is globally attracting stable node, which implies that the reefs are healthy. By increasing the fishing rate (for $f > f_1$), the macroalgae–parrotfish state becomes a stable node, which implies that macroalgae arise and reefs switch from healthy to unhealthy. When the fishing rate is in some intermediate range $0 < k < k_0$, then the interior state E^* is

unstable, but the coral–parrotfish state and the macroalgae–parrotfish state are both stable; however, if $k_0 < k < 1$, then the interior state E^* is stable, and the coral–parrotfish and macroalgae–parrotfish states are both unstable (see Figure 7).

In contrast, because it takes some time for algal turfs to arise after macroalgae are grazed by parrotfish, then the inherent time delay has significant impact on the dynamics of coral–algae–parrotfish interactions. Therefore, we have incorporated the delay in our model and treated both the fishing effort and the time delay as the bifurcation parameters. Delay has no effect on the stability of the extinction state, macroalgae only state, coral only state, and parrotfish only state. However, stability of the coral–parrotfish state and the macroalgae–parrotfish state depends not only on the fishing effort but also on the time delay. Reefs remain healthy only for a low fishing rate and a short delay time. With high fishing rate and a long delay time, the macroalgae–parrotfish state is stable, and hence the healthy reefs switch to the macroalgae-dominant status.

For some critical values of the time delay, a Hopf bifurcation occurs, which leads to a nontrivial periodic solution. This implies a switch between healthy and unhealthy states. This phenomenon can only appear in the DDE model. For large enough time delay, oscillations with large amplitudes appear. Finally, some numerical simulations are carried out for illustrating the analytic results.

REFERENCES

Bellwood, D. R., Hughes, T. P., Folke, C., & Nystrom, M. (2004). Confronting the coral reef crisis. *Nature*, *429*, 827–833.

Blackwood, J. C., & Hastings, A. (2011). The effect of time delays on Caribbean coral–algal interactions. *Journal of Theoretical Biology*, *273*, 37–43.

Blackwood, J. C., Hastings, A., & Mumby, P. J. (2012). The effect of fishing on hysteresis in Caribbean coral reefs. *Theoretical Ecology*, *5*, 105–114.

Chen, F. D. (2005). On a nonlinear nonautonomous predator–prey model with diffusion and distributed delay. *Journal of Computational and Applied Mathematics*, *180*(1), 33–49.

Cooke, K. L., & Grossman, Z. (1982). Discrete delay, distributed delay and stability switches. *Journal of Mathematical Analysis and Applications*, *86*, 592–627.

Gard, T. C., & Hallam, T. G. (1979). Persistence in food web—1, Lotka–Volterra food chains. *Bulletin of Mathematical Biology*, *41*, 877–891.

Hughes, T. P., Baird, A. H., & Bellwood, D. R. (2003). Climate change, human impacts, and the resilience of coral reefs. *Science*, *301*, 929–933.

Hutson, V. (1986). A theorem on average Liapunov functions. *Monatshefte für Mathematik*, *98*, 267–275.

Li, X., Wang, H., Zhang, Z., & Hastings, A. (2014). Mathematical analysis of coral reef models. *Journal of Mathematical Analysis and Applications*, *416*, 352–373.

Mumby, P. J. (2006). The impact of exploiting grazers (Scaridae) on the dynamics of Caribbean coral reefs. *Ecological Applications*, *16*, 747–769.

Mumby, P. J., Foster, N. L., & Glynn Fahy, E. A. (2005). Patch dynamics of coral reef macroalgae under chronic and acute disturbance. *Coral Reefs*, *24*, 681–692.

Mumby, P. J., Hastings, A., & Edwards, H. J. (2007). Thresholds and the resilience of Caribbean coral reefs. *Nature*, *450*, 98–101.

Pandolfi, J. M., Bradbury, R. H., & Sala, E. (2003). Global trajectories of the long-term decline of coral reef ecosystems. *Science*, *301*, 955–958.

How to cite this article: Fattahpour H, Zangeneh HRZ, Wang H. Dynamics of coral reef models in the presence of parrotfish. *Natural Resource Modeling*. 2019;32:e12202. https://doi.org/10.1111/nrm.12202